



Generation of squeezed light vacuum enabled by coherent population trapping

P. NEVEU,¹ J. DELPY,¹ S. LIU,¹ C. BANERJEE,¹ J. LUGANI,¹  F. BRETENAKER,^{1,2}  E. BRION,³ AND F. GOLDFARB^{1,*} 

¹Université Paris-Saclay, CNRS, Ecole Normale Supérieure Paris-Saclay, CentraleSupélec, LuMin, Gif-sur-Yvette, France

²Light and Matter Physics Group, Raman Research Institute, Bangalore, India

³CNRS, Université de Toulouse III Paul Sabatier, LCAR, IRSAMC, Toulouse, France

*fabienne.goldfarb@universite-paris-saclay.fr

Abstract: We demonstrate the possibility to generate squeezed vacuum states of light by four wave mixing (FWM) enabled coherent population trapping in a metastable helium cell at room temperature. Contrary to usual FWM far detuned schemes, we work at resonance with an atomic transition. We investigate the properties of such states and show that the noise variances of the squeezed and anti-squeezed quadratures cannot be explained by the simple presence of losses. A specific model allows us to demonstrate the role played by spontaneous emitted photons, which experience squeezing while propagation inside of the cell. This theoretical model, which takes into account both residual absorption and spontaneous emission, leads to an excellent agreement with the experimental data without any adjusted parameter.

© 2021 Optical Society of America under the terms of the [OSA Open Access Publishing Agreement](#)

1. Introduction

Squeezed states are the simplest example of non-classical states of light. Although still Gaussian, such states can turn out to be a strong asset in many applications such as high sensitivity spectroscopy, low noise optical amplification and signal processing, improved sensors, new imaging techniques, magnetometry or quantum information protocols with continuous variables [1–9]. While the first recorded squeezed state, generated via four wave mixing in a sodium vapor, was only 0.3 dB below the vacuum noise [10], investigations for improved systems and non-linear phenomena progressively led to much higher squeezing rates: the state of the art squeezing of 15 dB was achieved some years ago in an optical parametric amplifier operating below threshold, for calibration of photoelectric efficiency [11]. In Rubidium vapor cells, about 8.8 dB of intensity-difference squeezing has been obtained [12]. However, such states can be destroyed by unwanted processes, which might limit their potential : this is why these experiments are performed far from atomic resonances in order to avoid absorption.

We have recently demonstrated in [13] that coherent population trapping (CPT) occurring along the $|2^3S_1\rangle \leftrightarrow |2^3P_1\rangle$ (D_1) transition of metastable helium can enhance the non-linearity induced by the nearby $|2^3S_1\rangle \leftrightarrow |2^3P_2\rangle$ (D_2) transition, leading to a very efficient four-wave mixing (FWM) process. The configuration used below is very different from the more usual far detuned schemes: the light here is resonant with an atomic transition, and nonlinear processes can be efficient thanks to the narrow transparency window opened by the CPT process. Classical parametric gains as large as 9 dB, for an optical depth lower than 5 (on the D_1 line), have then been obtained. One naturally expect such a large phase sensitive gain to open the door to the generation of strongly squeezed states of light. The aim of the present paper is thus to experimentally explore this potentiality, while paying particular attention to the losses induced by the residual absorption from the D_2 transition and to the associated spontaneous emission. In particular, we aim at carefully characterizing the generated squeezed states in order to demonstrate the effect of the photons, which are re-emitted spontaneously into the mode probed by the homodyne

detection, and to compare the measurements with a complete model describing the propagation of the incident vacuum state into the atomic vapor.

2. Experiment

Figure 1 shows a schematic of the experimental setup. Helium atoms are pumped into their metastable state 2^3S_1 by means of an electrical discharge at 80 MHz (RF), leading to a density of metastable helium atoms He^* of about $2 \times 10^{11} \text{ cm}^{-3}$. A fiber laser at $1.083 \mu\text{m}$, resonant with the D_1 transition of He^* , is split into a driving pump beam and a local oscillator (LO) using a polarizing beamsplitter (PBS). The pump beam, of Rabi frequency Ω , is then sent to another PBS, which allows the vacuum probe $|0\rangle$ to enter through its other input port: the probed mode is thus polarized orthogonally to the driving field. While propagating inside the helium cell, the vacuum state with the same frequency and spatial mode as the pump experiences four-wave mixing (FWM) inside the medium [13] before being efficiently separated from the transmitted pump by a Glan-Taylor polarizer. It is then sent to the homodyne detection part and recombined with the local oscillator, which was previously reflected by a mirror mounted on a piezoelectric transducer (PZT) to allow its phase to be scanned. The power spectral densities (PSD) of the different quadratures are recorded using an electrical spectrum analyzer (ESA).

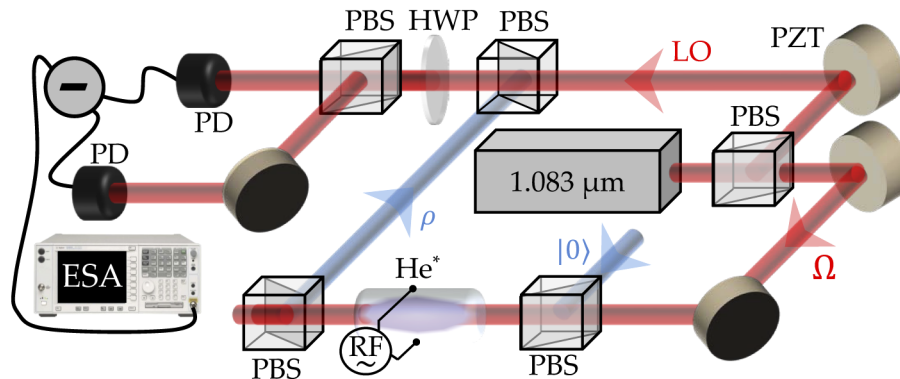


Fig. 1. Experimental setup. The pump driving beam Ω and the local oscillator (LO) are derived from the same laser. PZT: piezoelectric transducer allowing to scan the LO phase. PBS: polarization beam splitter. $|0\rangle$, ρ : input and output probe field states. ESA: Electrical spectrum analyzer. PD: photodiodes. HWP: half-wave plate. RF: radiofrequency discharge.

The linearly polarized pump is the coherent sum of a right and a left circular polarizations. Figure 2 shows the different transitions excited by the two linearly polarized pump and probe beams and the relevant atomic sublevels of the 2^3P_1 and 2^3P_2 states. The $3P_0$ state, which is 29.6 GHz above the $3P_1$, is far enough to be neglected, and thus not shown here. Because of the selection rules, the D_1 transition constitutes an excellent Λ -like atomic system [14]. This allows the excitation of Raman coherences with a high efficiency, inducing a strong transparency of the medium due to CPT. It leads to an enhancement of the non-linearities experienced by a weak and orthogonally polarized probe beam through FWM processes via the closest neighbouring transition $|2^3S_1\rangle \leftrightarrow |2^3P_2\rangle$ (D_2 transition). These large nonlinearities, associated with small losses, make it possible to achieve classical parametric gains as large as 9 dB for optical depths of the order 4.5 [13]. Such phase sensitive parametric gain is expected to be associated with squeezed states of light.

When the input probe beam consists of vacuum, we thus expect to generate a strongly squeezed vacuum state. Figure 3 shows a measurement of the vacuum noise PSD at 150 kHz as a function of time when the LO phase is linearly and slowly scanned at a rate close to 1 rad/s. This noise

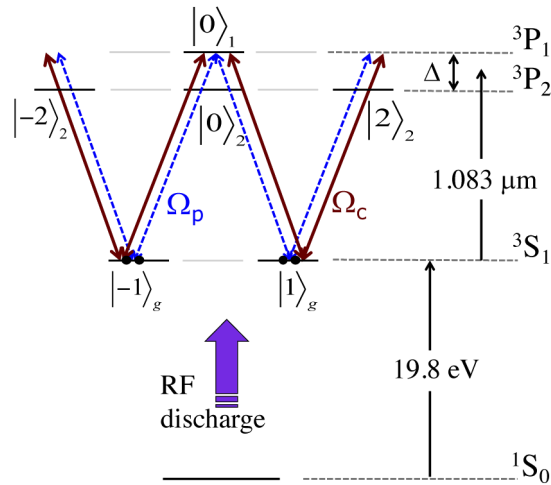


Fig. 2. Level structure of metastable ^4He . Full blue line (dashed red line): excitation paths by the linearly polarized strong coupling (weak probe) beam of Rabi frequency Ω_C (Ω_P). The levels are labeled by the value of the projection of the total angular momentum m along the propagation direction of light. Only relevant Zeeman sublevels are shown in black lines. The other ones are in gray lines.

measurement is performed using a carefully balanced detection followed by a spectrum analyzer (Agilent EXA N 9010A). We have checked that our measurements are shot noise limited. The frequency at which the light quadrature noises are measured (150 kHz) is chosen such that it is larger than the bandwidth of residual low frequency noises of technical origin, but within the bandwidth of the power broadened CPT occurring in He^* , which is evaluated to be between 500 and 800 kHz in our experimental conditions [13]. The nearly horizontal full blue line was recorded in the absence of any pump field, and provides the standard quantum limit (SQL). The red periodic signal was obtained with a pump power of 50 mW, which leads to the maximal parametric gain of about 9 dB. A perfect squeezer associated with such a parametric gain should

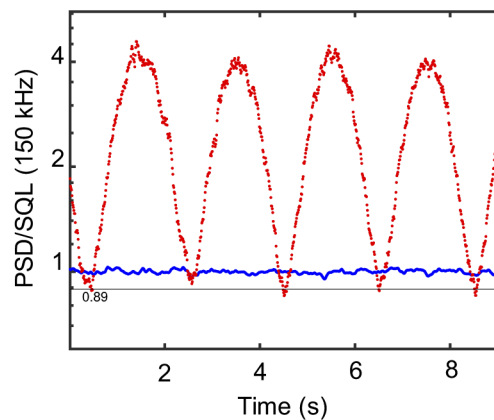


Fig. 3. Quadrature noise at 150 kHz measured while the phase of the LO is scanned. Blue line: calibration of the standard quantum limit (SQL) in the absence of pump beam. Red line: Vacuum noise in the presence of a 55 mW pump beam. The minimum noise is equal to 0.89 times the SQL, corresponding to 0.51 dB of squeezing.

lead to the green full line curve of Fig. 4, i. e., a variation of the noise PSD of the different quadratures between -9 dB to $+9$ dB around the SQL. However, the noise PSD we measure varies only from -0.51 dB below the SQL to $+7.0$ dB over the SQL.

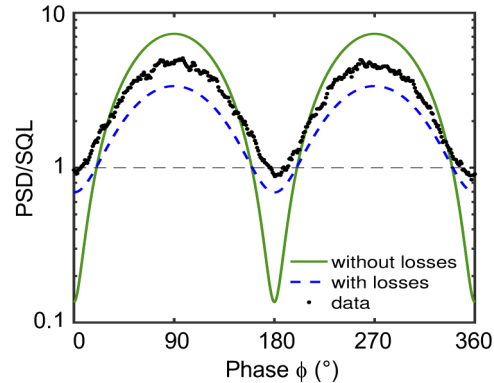


Fig. 4. Evolution of the quadrature noise versus phase of the local oscillator. Black dots: measurements. Green full line: theory, perfect squeezer with $\zeta = 1$. Blue dashed line: theory, taking into account detection losses ($\approx 42\%$) and residual absorption by the D_2 line ($\approx 37\%$).

Such noise levels cannot be explained only by the losses experienced by the squeezed vacuum state. Indeed, the pure squeezer (green full line in Fig. 4) is reduced to the blue dashed curve in the same figure if we take into account i) the losses induced by the cell windows (92% transmission), which are not anti-reflection coated, ii) the imperfect transmission of the optics located after the cell (81% transmission), iii) the limited quantum efficiency (78%, evaluated from the response of the photodiodes given by datasheet) of the balanced detection, and iv) the residual absorption of the atoms (about 37% absorption). Taking all these sources of losses, which were determined by appropriate measurement, the blue dashed curve in Fig. 4 predicts a noise increase of 5.2 dB along the amplified quadrature and a noise squeezing of -1.6 dB along the de-amplified quadrature, in strong disagreement with the measured values (black dots). This

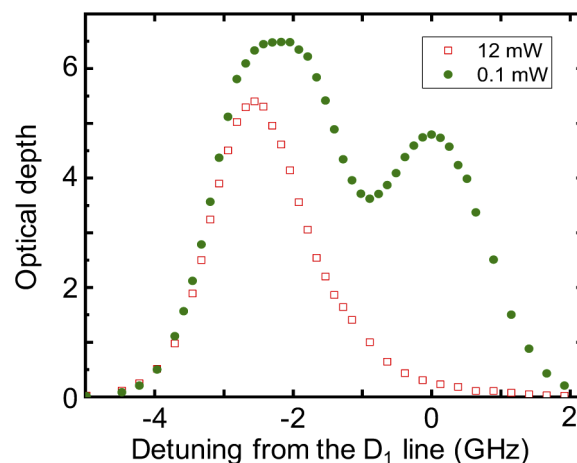


Fig. 5. Absorption spectra obtained for a pump power of 0.1 mW (filled green circles) and 12 mW (empty red squares). Notice the residual absorption at the center of the D_1 line due to the D_2 line, even in the presence of CPT.

discrepancy cannot be compensated for by adding more losses on the probe channel. Indeed, such extra losses would decrease the values of both the squeezing and the “anti-squeezing”, and worsen the discrepancy between theory and experiment. We thus explore whether the experimental results can be understood by taking into account some residual spontaneous emission falling in the probe mode. Before describing the model that renders account of the role of this spontaneous emission (see section 3 below), Fig. 5 reproduces the small-signal absorption spectrum of the cell for two different pump powers. It shows that apart from the imperfect CPT phenomenon, which does not completely cancel absorption from the D_1 transition, the D_2 transition is close enough to the D_1 transition to be also responsible for some residual absorption. This pump absorption promotes a small fraction of the atoms to the upper level, from which they can decay by spontaneously emitting photons, a fraction of which can fall into the probe mode. As we see in the next section, this emission strongly increases the value of the anti-squeezing along the amplified quadrature, while the squeezing value along the de-amplified quadrature is much less altered.

3. Model

We model the spontaneous emission falling in the probe mode in the following manner. If ε is the probability for one spontaneously emitted photon to fall into the considered vacuum mode, then, in the absence of any other effect (such as losses or squeezing), the mode field is in the following thermal mixed state

$$\rho_{\text{th}} = (1 - \varepsilon) \sum_k \varepsilon^k |k\rangle \langle k|. \quad (1)$$

The mean photon number in such a state is $\bar{n} = \text{Tr}(a^\dagger a \rho_{\text{th}}) = \varepsilon/(1 - \varepsilon)$ and the variance of any quadrature X_ϕ is $\text{Tr}[\rho_{\text{th}} X_\phi^2] - \text{Tr}[\rho_{\text{th}} X_\phi]^2 = \text{SQL} \times (1 + 2\bar{n})$.

To model the propagation of the input vacuum state through the helium cell, we discretize the medium in thin slices of thickness dz . The state $\rho(z + dz)$ of the field at the output of such a slice is computed as a function of the state $\rho(z)$ of the input one, under the action of squeezing, absorption, and spontaneous emission.

Squeezing is described by the well-known operator $S(\zeta)$ given by:

$$S(\zeta) = \exp\left[\frac{\zeta a^2 - \zeta^* a^{\dagger 2}}{2}\right]. \quad (2)$$

The overall squeezing parameter ζ is considered to be real and can be evaluated through phase sensitive amplification experiments. To fit our experiments we use the value $\zeta = 1.0$, which was deduced from previously recorded values of the phase sensitive gain [13]. The elementary operator acting on an infinitesimal slice of width dz is given by:

$$S(d\zeta) \approx 1 + d\zeta (a^2 + a^{\dagger 2})/2. \quad (3)$$

The quantity $d\zeta$ is related to the thickness of the slice located at abscissa z by:

$$d\zeta = \frac{\sinh \zeta}{\sqrt{1 + (1 - \frac{\varepsilon}{L})^2 \sinh^2 \zeta}} \frac{dz}{L}, \quad (4)$$

where L is the length of the cell. The output field resulting from the action of this elementary squeezer is the given by the following unitary transformation

$$\rho(z + dz) = S(d\zeta) \rho(z) S^\dagger(d\zeta). \quad (5)$$

Absorption in the medium reduces the mean number of photons and destroys coherent superpositions between photon number states. We model this effect using a superoperator

$\mathcal{D}(\rho, \kappa)$ acting on a state ρ in the presence of an absorption coefficient κ such that

$$\begin{cases} \rho_{nm} \rightarrow (1 - \kappa n)\rho_{nm} + \kappa(n+1)\rho_{n+1,n+1}, \\ \rho_{nm} \rightarrow (1 - \kappa(n+m)/2)\rho_{nm} - \sqrt{n+1}\sqrt{m+1}\rho_{n+1,m+1}. \end{cases} \quad (6)$$

These expressions mean that we restrict to the annihilation of only one photon, transforming a state $|n\rangle$ into $|n-1\rangle$. This approximation is valid as soon as the absorption is small, i. e. $\kappa \ll 1$, which is obtained by considering thin enough elementary slices. This transformation corresponds to the so-called Bernoulli transformation [15,16] in the weak losses limit. If κ corresponds to the attenuation through a slice of thickness dz , the action of this slice on the state ρ of the field reads

$$\rho(z + dz) = \mathcal{D}(\rho(z), 1 - dT), \quad (7)$$

where $dT = T^{dz/L}$ is the slice transmission.

In the experiment, the value of \bar{n} depends on the position z inside the cell : $\bar{n}(z + dz) = \bar{n}(z) + d\bar{n}$, where $d\bar{n}$ is the small average number of photons added within each slice. Spontaneously emitted photons are added incoherently to the input field, so that

$$\rho(z + dz) = \alpha\rho(z) + \beta d\bar{n}a^\dagger\rho(z)a. \quad (8)$$

In Eq. (8), the slices are supposed to be sufficiently thin to consider addition of no more than one photon to the state ρ , and the α and β coefficients allow to preserve the normalization $\text{Tr}[\rho(z + dz)] = 1$.

If the spontaneous emission rate is supposed to be proportional to the local absorption coefficient, the distribution of the equivalent thermal photon number $\bar{n}(z)$ is related to the global quantity $\bar{n}(L)$ at the output of the cell through:

$$\bar{n}(z) = \bar{n}(L) \frac{z}{L} T^{\frac{z}{L}-1}. \quad (9)$$

In order to measure $\bar{n}(L)$, we use the following calibration method. We slightly misalign the coupling beam, by an angle of the order of 1° , leading to the fact that the mode detected by the balanced homodyne detection, does no longer experience CPT and squeezing. Since spontaneous emission can be supposed to be isotropic, this small misalignment does not modify the value of ε . We then measure the variance of the quadrature noise in these conditions. Figure 6 shows a measurement of the evolution of this quadrature variance, normalized to the SQL, as a function of the absorbed pump power. This calibration experiment permits us to relate the values of ε and $\bar{n}(L)$ to the amount of absorbed pump power, a quantity which is easy to measure at any time during the experiment. Taking into account the transmission T_d of the part of the experiment located between the cell and the homodyne detection, the average number of photons reaching the detector becomes $\bar{n}_{\text{meas}} = T_d\bar{n}(L)$. We can then perform simulations taking both spontaneous emission and losses into account. This leads to the orange full line in Fig. 7, which is in excellent agreement with the measurements (black dots). Comparison with the former calculation taking only losses into account (dashed blue line) shows that the effect of spontaneous emission is to globally increase the maximum value of the noise. However, it leaves the value of the noise PSD along the squeezed quadrature almost unchanged. The agreement between our model and the measurements is all the more remarkable, due to the fact that all the values of the parameters used in the simulations have been obtained from measurements without any adjustment. It should be noticed that a good agreement between theory and experiment cannot be obtained just by a simple translation of the dashed blue curve. If one vertically translates the dashed blue curve in such a way that its maximum coincides with the maximum measured noise level (+7.0 dB), then its minimum would be above the SQL by 0.2 dB. This proves that one cannot overlook the fact that spontaneously emitted photons experience some squeezing. The remaining discrepancy between the measurements and the full orange line around the noise minimum is probably due to the part of spontaneous emission which is too far detuned and thus does not experience squeezing.

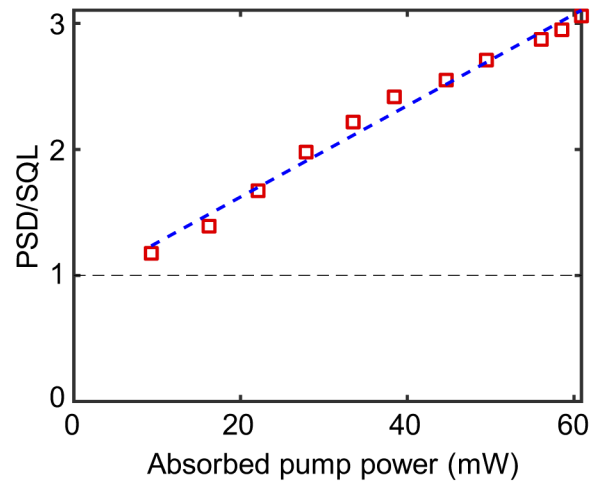


Fig. 6. Calibration of spontaneous emission falling in the detected mode. Red squares: measured noise PSD versus absorbed pump power with slightly misaligned pump beam. Blue dashed line: linear fit. Horizontal dashed line: SQL.

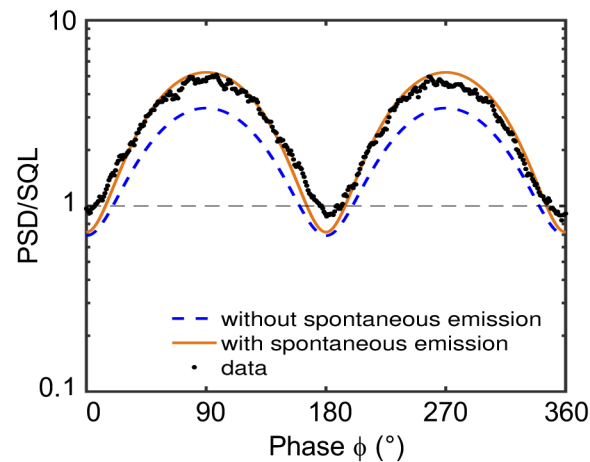


Fig. 7. Evolution of the quadrature noise versus phase of the local oscillator. Black dots: measurements. Blue dashed line: theory, taking into account detection losses and residual absorption by the D_2 line. Orange full line: complete model, taking also spontaneous emission into account with $\bar{n} = 0.23$.

4. Conclusion

We have experimentally demonstrated the generation of squeezed vacuum states of light by CPT enabled four-wave mixing in metastable helium atoms at room temperature. The configuration that we used is very different from usual far detuned schemes: the light is here resonant with an atomic transition, and nonlinear processes are made efficient thanks to the narrow transparency window opened by the CPT process. Thanks to the simple level structure of helium, we could also model this phenomenon and its limitations. Indeed, this method should in principle be able to provide strongly squeezed states even with a quite low optical depth. However, in the case of metastable helium atoms at room temperature, the amount of squeezing is limited by spontaneous emission. We have developed a theoretical model, which fairly reproduces the experimental data,

and proves how the thermal redistribution induced by spontaneous emission alters the squeezed states. In particular, it leads to a strong increase of the noise variance of the amplified quadrature. It should be also emphasized that our model explains why the final amount of squeezing at the end of the cell is not negligible, thanks to the squeezing experienced by the new state obtained by adding spontaneous emission to the input vacuum.

As far as we know, these results are the first ones obtained in resonant conditions: the squeezing rate is not as high as the ones obtained with far detuned systems, but our model predicts that improved amounts of squeezing could be achieved with a better optimized system, in which residual absorption would be decreased either by selecting a narrower line or a larger separation between the CPT system and the transition used for the four wave mixing processes.

Three-level systems, such as the Λ -system considered here, are known to allow reversible mapping of quantum states between light and atoms [17,18]. The phenomena that we have described here involve superpositions of atomic states and should thus be associated with strongly squeezed collective spin states [19], which are attractive for precision metrology [20]. It could thus be interesting to probe these atomic states, for example by spin noise spectroscopy techniques [21,22].

Funding. Laboratoire d'excellence Physique Atomes Lumière Matière; DIM Nano-K; Institut Universitaire de France.

Disclosures. The authors declare no conflicts of interest.

References

1. E. S. Polzik, J. Carri, and H. J. Kimble, "Spectroscopy with squeezed light," *Phys. Rev. Lett.* **68**(20), 3020–3023 (1992).
2. R. Slavík, F. Parmigiani, J. Kakande, C. Lundström, M. Sjödin, P. A. Andrekson, R. Weerasuriya, S. Sygletos, A. D. Ellis, L. Grüner-Nielsen, D. Jakobsen, S. Herstrøm, R. Phelan, J. O'Gorman, A. Bogris, D. Syvridis, S. Dasgupta, P. Petropoulos, and D. J. Richardson, "All-optical phase and amplitude regenerator for next-generation telecommunications systems," *Nat. Photonics* **4**(10), 690–695 (2010).
3. Z. Tong and S. Radic, "Low-noise optical amplification and signal processing in parametric devices," *Adv. Opt. Photonics* **5**(3), 318–384 (2013).
4. M. A. Taylor, J. Janousek, V. Daria, J. Knittel, B. Hage, H.-A. Bachor, and W. P. Bowen, "Biological measurement beyond the quantum limit," *Nat. Photonics* **7**(3), 229–233 (2013).
5. N. Otterstrom, R. C. Pooser, and B. J. Lawrie, "Nonlinear optical magnetometry with accessible in situ optical squeezing," *Opt. Lett.* **39**(22), 6533–6536 (2014).
6. V. Boyer, A. M. Marino, R. C. Pooser, and P. D. Lett, "Entangled images from four-wave mixing," *Science* **321**(5888), 544–547 (2008).
7. F. Acernese, M. Agathos, L. Aiello, A. Allocca, A. Amato, S. Ansoldi, S. Antier, M. Arène, N. Arnaud, S. Ascenzi, and P. Astone, "Increasing the astrophysical reach of the advanced virgo detector via the application of squeezed vacuum states of light," *Phys. Rev. Lett.* **123**(23), 231108 (2019).
8. M. Tse, H. Yu, N. Kijbunchoo, A. Fernandez-Galiana, P. Dupej, L. Barsotti, C. D. Blair, D. D. Brown, S. E. Dwyer, A. Effler, and M. Evans, "Quantum-enhanced advanced ligo detectors in the era of gravitational-wave astronomy," *Phys. Rev. Lett.* **123**(23), 231107 (2019).
9. H. Yonezawa and A. Furusawa, "Continuous-variable quantum information processing with squeezed states of light," *Opt. Spectrosc.* **108**(2), 288–296 (2010).
10. R. E. Slusher, L. W. Hollberg, B. Yurke, J. C. Mertz, and J. F. Valley, "Observation of squeezed states generated by four-wave mixing in an optical cavity," *Phys. Rev. Lett.* **55**(22), 2409–2412 (1985).
11. H. Vahlbruch, M. Mehmet, K. Danzmann, and R. Schnabel, "Detection of 15 db squeezed states of light and their application for the absolute calibration of photoelectric quantum efficiency," *Phys. Rev. Lett.* **117**(11), 110801 (2016).
12. C. F. McCormick, A. M. Marino, V. Boyer, and P. D. Lett, "Strong low-frequency quantum correlations from a four-wave-mixing amplifier," *Phys. Rev. A* **78**(4), 043816 (2008).
13. P. Neveu, C. Banerjee, J. Lugani, F. Bretenaker, E. Brion, and F. Goldfarb, "Phase sensitive amplification enabled by coherent population trapping," *New J. Phys.* **20**(8), 083043 (2018).
14. F. Goldfarb, J. Ghosh, M. David, J. Ruggiero, T. Chanelière, J.-L. Le Gouët, H. Gilles, R. Ghosh, and F. Bretenaker, "Observation of ultra-narrow electromagnetically induced transparency and slow light using purely electronic spins in a hot atomic vapor," *Europhys. Lett.* **82**(5), 54002 (2008).
15. A. Lvovsky, "Iterative maximum-likelihood reconstruction in quantum homodyne tomography," *J. Opt. B: Quantum Semiclassical Opt.* **6**(6), S556–S559 (2004).
16. U. Leonhardt, *Measuring the quantum state of light*, vol. 22 (Cambridge university press, 1997).
17. M. Fleischhauer and M. D. Lukin, "Dark-state polaritons in electromagnetically induced transparency," *Phys. Rev. Lett.* **84**(22), 5094–5097 (2000).

18. M. D. Lukin, S. F. Yelin, and M. Fleischhauer, "Entanglement of atomic ensembles by trapping correlated photon states," *Phys. Rev. Lett.* **84**(18), 4232–4235 (2000).
19. J. Hald, J. Sorensen, C. Schori, and E. Polzik, "Spin squeezed atoms: A macroscopic entangled ensemble created by light," *Phys. Rev. Lett.* **83**(7), 1319–1322 (1999).
20. D. Döring, G. McDonald, J. E. Debs, C. Figl, P. A. Altin, H.-A. Bachor, N. P. Robins, and J. D. Close, "Quantum-projection-noise-limited interferometry with coherent atoms in a ramsey-type setup," *Phys. Rev. A* **81**(4), 043633 (2010).
21. V. S. Zapasskii, "Spin-noise spectroscopy: from proof of principle to applications," *Adv. Opt. Photonics* **5**(2), 131–168 (2013).
22. N. A. Sinitsyn and Y. V. Pershin, "The theory of spin noise spectroscopy: a review," *Rep. Prog. Phys.* **79**(10), 106501 (2016).